PHYSICAL REVIEW A **90**, 052515 (2014)

Determination of small level splittings in highly charged ions via angle-resolved measurements of characteristic x rays

Z. W. Wu,[1,2] N. M. Kabachnik,[3,4] A. Surzhykov,[1] C. Z. Dong,[2] and S. Fritzsche[1,5]

[1]*Helmholtz-Institut Jena, Fröbelstieg 3, D-07743 Jena, Germany*

[2]*Key Laboratory of Atomic and Molecular Physics & Functional Materials of Gansu Province, College of Physics and Electronic Engineering, Northwest Normal University, Lanzhou 730070, People's Republic of China*

[3]*European XFEL, Albert-Einstein-Ring 19, D-22761 Hamburg, Germany*

[4]*Skobeltsyn Institute of Nuclear Physics, Lomonosov Moscow State University, Moscow 119991, Russia*

[5]*Theoretisch-Physikalisches Institut, Friedrich-Schiller-Universität Jena, Max-Wien-Platz 1, D-07743 Jena, Germany*

(Received 1 October 2014; published 18 November 2014)

The angular distribution and the photon-photon angular correlation have been investigated for the x-ray emission from two-step radiative cascades that proceed via *overlapping* intermediate resonances. In particular, density matrix theory is applied in order to explore how the splitting of these intermediate levels affects the subsequent x-ray emission and whether measurements of photon angular distributions may help reveal level crossings in highly charged ions, if analyzed along isoelectronic sequences. Detailed computations within the multiconfiguration Dirac-Fock method were performed especially for the two-step $1s2p^2\ J_i = 1/2,3/2 \rightarrow 1s2s2p\ J = 1/2,3/2 + \gamma_1 \rightarrow 1s^22s\ J_f = 1/2 + \gamma_1 + \gamma_2$ cascade of lithiumlike ions, for which a level crossing of the two $1s2s2p\ J = 1/2,3/2$ intermediate resonances occurs in the range $74 \leqslant Z \leqslant 79$. For this cascade, a remarkably strong depolarization effect, associated with the finite lifetime of these intermediate levels, is found for the angular distribution and the photon-photon correlation function for all level splittings $\Delta\omega \lesssim 0.2$ a.u. ≈ 5.4 eV. We therefore suggest that accurate angle-resolved measurements of the x-ray emission may serve also as a tool for determining small level splittings in excited highly charged ions.

DOI: 10.1103/PhysRevA.90.052515 PACS number(s): 31.10.+z, 31.15.aj

I. INTRODUCTION

Highly charged ions (HCIs) are known as a unique tool for studying the interaction of strong electromagnetic fields with matter. In particular the x-ray emission from these ions have been investigated for many years, both experimentally [1–4] and theoretically [5,6]. These investigations helped reveal many details about the structure and dynamics of HCIs [7–9]. Recently, moreover, studies on the angular distribution and linear polarization of these x rays provided even further insights into the electron-electron [10–13], electron-photon [14–16], and electron-nucleus interactions [17,18]. A particularly strong effect of the Breit interaction on the x-ray emission was found, for example, for the angular distribution and linear polarization of the $1s2s^22p_{1/2}\ J = 1 \rightarrow 1s^22s^2\ J = 0$ fluorescence line of highly charged berylliumlike ions following the dielectronic recombination [19,20] or electron-impact excitation [21], respectively. Finally, the influence of the hyperfine interaction upon the angular and polarization properties of the emitted x rays from HCIs was analyzed and found unexpectedly strong, even if the fine and hyperfine structure of these lines cannot be resolved [22,23].

Until the present, however, almost all experimental and theoretical studies on the angular distribution of x rays were performed for photons emitted from well-isolated fine-structure levels. Little attention has been paid so far to x-ray emission cascades that proceed via two (or more) overlapping intermediate resonances. When compared with isolated levels, the x-ray emission via overlapping resonances is affected also by spin-spin or spin-orbit interactions that may lead to a *depolarization* of the intermediate levels because of their finite lifetimes. A polarization of the intermediate resonances often arises if the initial resonance of a two-step radiative cascade was polarized (usually aligned), e.g., in the process of dielectronic recombination or electron impact excitation. If no further details are known about the exact time interval between the subsequent emission processes in the cascade, this depolarization can be characterized by means of so-called depolarization factors that just depend on the energy splitting and the natural width of the intermediate resonances [24,25]. This effect of partially overlapping resonances upon the emission of photons and electrons has been termed also *lifetime-induced depolarization* in the literature.

Most work on this depolarization effect has been performed so far for the angular distribution of electrons or for electron-electron correlations that arise in the photoionization of atoms in strong light fields [25,26] or in the decay of inner-shell excited atoms and ions [27–29]. In the two-photon double ionization (2PDI) process of atoms, however, the depolarization factors will depend not only on the widths and energy splitting of the overlapping and coherently excited resonances but also on the duration of the laser pulse [25]. For two-step x-ray emission cascades via overlapping intermediate resonances in HCIs, in contrast, the lifetime-induced depolarization can be characterized merely by the width and energy splitting of these resonances. We therefore expect that the photon-photon angular correlation function and the angular distribution of the second-step photons will be affected by the level splitting of the overlapping resonances and that this effect on the x-ray emission of HCIs might become measurable near to the crossing of levels along some given isoelectronic sequence.

In this contribution, we study theoretically the x-ray emission in two-step radiative cascades of HCI with

overlapping intermediate resonances. In particular, we here consider two scenarios: (i) Coincidence measurements of the two subsequently emitted photons and (ii) measurements of just the second-step photon, where the first photon remains unobserved. To this end, density matrix theory is applied in order to obtain general expressions for the angular correlation function and angular distribution of the emitted photons. Emphasis in this work is placed especially upon the role of the lifetime-induced depolarization and how the energy splitting of the overlapping resonances affects the x-ray emission. However, while the formalism below can be applied to general atoms and ions, independent of their particular shell structure, we here consider the $1s2p^2\ J_i = 1/2,3/2 \to 1s2s2p\ J = 1/2,3/2 + \gamma_1 \to 1s^2 2s\ J_f = 1/2 + \gamma_1 + \gamma_2$ two-step cascade along the lithium isoelectronic sequence. These ions have a relatively simple level structure and exhibit a level crossing of the two $1s2s2p\ J = 1/2,3/2$ intermediate resonances in the range $74 \leqslant Z \leqslant 79$. For this cascade, moreover, a particular strong effect of the level splitting and the alignment of the initial $1s2p^2\ J_i = 3/2$ resonance is found in our computations for the angular distribution of the emitted x-ray photons. We therefore suggest that accurate measurements on the x-ray emission may serve also as a tool for determining small splittings in the level structure of excited HCIs.

The paper is structured as follows. In the next section, expressions are derived for the photon-photon angular correlation function as well as the angular distribution of the individual photons within density matrix theory. These expressions are then applied and analyzed especially for the radiative decay of lithiumlike ions, along with a brief account on the computations. In Sec. III, we then discuss the anisotropy parameters as well as the predicted angular distribution and angular correlation function. Finally, a few conclusions of the present work are given in Sec. IV.

Atomic units are used throughout this paper unless stated otherwise.

II. THEORY AND COMPUTATION

Let us consider the two-step decay cascade

$$A^{q+**}(\alpha_i J_i) \to \gamma_1 + \left\{ \begin{matrix} A^{q+*}(\alpha J) \\ A^{q+*}(\alpha' J') \end{matrix} \right\} \to \gamma_1 + \gamma_2 + A^{q+}(\alpha_f J_f), \qquad (1)$$

where a q-fold charged ion A^{q+**} is initially assumed to be in the doubly excited level $\alpha_i J_i$. In the first step of the cascade, the two overlapping intermediate resonances αJ and $\alpha' J'$ are populated coherently due to the emission of the first photon γ_1. The fast emission of a subsequent second photon γ_2 brings the ion into its ground level $\alpha_f J_f$, as shown schematically also in Fig. 1. Here, J_i, J, J' and J_f are the total angular momenta of the corresponding levels, while α_i, α, α', and α_f refer to all further quantum numbers as required for a unique specification of the levels.

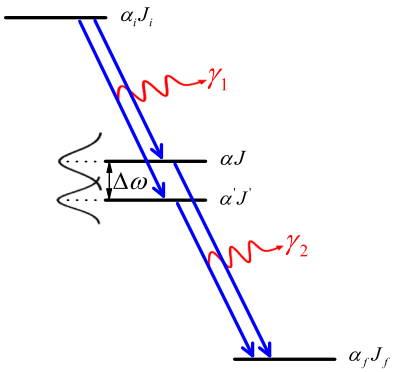

FIG. 1. (Color online) Level scheme of the two-step radiative decay cascade (1). The ion is initially assumed to be in the doubly excited level $\alpha_i J_i$ and decays radiatively via the two overlapping intermediate resonances αJ and $\alpha' J'$ into the ground level $\alpha_f J_f$. While the two photons γ_1 and γ_2 can be distinguished energetically, no further line structures could be resolved individually because of the (partial) overlap of the levels αJ and $\alpha' J'$.

A. Photon-photon angular correlation function

In analyzing the x-ray emission from HCIs, the formation and subsequent decay of the isolated excited states are usually described separately; cf. Refs. [30–32]. Therefore, not much needs to be said here about the excitation process, and we shall begin our analysis of process (1) simply in terms of the statistical tensors (state multipoles) $\rho_{k_i q_i}(\alpha_i J_i)$ as associated with the level $\alpha_i J_i$. These tensors fully characterize the polarization state of the initial ion as generated by some particular excitation process, and they also affect the properties of the subsequently emitted radiation. Therefore, we first briefly explain how the photon-photon angular correlation function can be expressed in terms of these tensors and the amplitudes for the subsequent photon emissions, but without going much into the details of the derivation.

When compared with other cascade processes, which proceed via isolated atomic levels, the major difference in dealing with *overlapping* intermediate resonances arises from their statistical tensors $\rho^{\rm ion}_{kq}(\alpha J, \alpha' J'; t)$. These tensors of the intermediate states evolve in time as $\sim \exp[(i\omega_{\alpha J, \alpha' J'} - \Gamma_{\alpha J, \alpha' J'})t]$ owing to spin-orbit interactions in the ion [25,26]. In the vector model of angular momenta, this evolution can be understood also as a precession of the total angular momentum of the ion around the quantization z axis (e.g., the direction of the electron beam) during the time interval between the first- and second-step photon emissions. However, since nothing is known about the exact time delay between the two-step emissions, we need to average the tensors $\rho^{\rm ion}_{kq}(\alpha J, \alpha' J'; t)$ over time. This average procedure gives rise to the so-called depolarization factors and to the time-averaged statistical tensors for the intermediate states of the photoion. Once we have derived the time-averaged statistical tensors, the photon-photon angular correlation function and the angular distribution of the photons can then be obtained by following standard lines of density matrix theory [33,34]. For example, the photon-photon angular correlation function is given as

follows:

$$W(\theta_1,\varphi_1;\theta_2,\varphi_2) = \sum_{k_i q_i \bar{k}\bar{q} k q} \sum_{\alpha J \alpha' J'} \sum_{\bar{p}\bar{L}\bar{p}'\bar{L}' p L p' L'} \rho_{k_i q_i}(\alpha_i J_i) \bar{M}_{\bar{p}\bar{L}} \bar{M}^*_{\bar{p}'\bar{L}'} M_{pL} M^*_{p'L'} (-1)^{L'+J+J_f+k} \langle kq, \bar{k}\bar{q} k_i q_i \rangle$$
$$\times \begin{Bmatrix} J' & L' & J_f \\ L & J & k \end{Bmatrix} \begin{Bmatrix} J & \bar{L} & J_i \\ J' & \bar{L}' & J_i \\ k & \bar{k} & k_i \end{Bmatrix} \varepsilon^{\mathrm{det}*}_{\bar{k}0}(\bar{p}\bar{L}, \bar{p}'\bar{L}') \varepsilon^{\mathrm{det}*}_{k0}(pL, p'L') h_{\alpha J, \alpha' J'} 4\pi Y_{\bar{k}\bar{q}}(\theta_1,\varphi_1) Y_{kq}(\theta_2,\varphi_2). \quad (2)$$

In this expression, we use the short-hand notations $\bar{M}_{\bar{p}\bar{L}} \equiv \langle \alpha J \| H_{\gamma_1}(\bar{p}\bar{L}) \| \alpha_i J_i \rangle$ and $M_{pL} \equiv \langle \alpha_i J_i \| H_{\gamma_2}(pL) \| \alpha J \rangle$ with the interaction Hamiltonian H_γ to denote the reduced transition amplitudes for the emission of the first- and second-step photons as well as the standard notations for the Clebsch-Gordan coefficients, the Wigner $6j$ and $9j$ symbols, and the spherical harmonics Y_{kq}, respectively. In this notation, moreover, the individual photons are characterized in terms of their multipolarity pL and with $p = 0$ in order to refer to the electric multipoles and $p = 1$ to the magnetic ones. There are two further entities that appear in the angular correlation function (2) for the case of the two overlapping resonances. The tensors $\varepsilon^{\mathrm{det}}_{k0}(pL, p'L')$ are here introduced in order to account for the efficiency of the detector setup for observing the individual photons with selected multipolarities pL and $p'L'$. They have their simplest form in the so-called *photon frame* [34],

$$\varepsilon^{\mathrm{det}}_{k0}(pL, p'L') = (-1)^{L'-1} \frac{\hat{L}\hat{L}'}{16\pi} \times \langle L1, L'-1 | k0 \rangle [1 + (-1)^f], \quad (3)$$

and with $f = L + p + L' + p' - k$ and $\hat{L} \equiv (2L+1)^{1/2}$, respectively. In addition, the depolarization factors are a consequence of the time-average procedure as outlined above. These factors can be expressed as [34]

$$h_{\alpha J, \alpha' J'} = \frac{\Gamma_{\alpha J, \alpha' J'} - i\omega_{\alpha J, \alpha' J'}}{\omega^2_{\alpha J, \alpha' J'} + \Gamma^2_{\alpha J, \alpha' J'}}, \quad (4)$$

and where $\omega_{\alpha J, \alpha' J'} = E_{\alpha J} - E_{\alpha' J'}$ refers to the splitting of the level energies and $\Gamma_{\alpha J, \alpha' J'} = \frac{1}{2}(\Gamma_{\alpha J} + \Gamma_{\alpha' J'})$ to the overall widths of the two overlapping resonances, with $\Gamma_{\alpha J}$ being the total width of level αJ. These depolarization factors also form a Hermitian matrix in which the diagonal matrix elements represent the incoherent contribution of the overlapping resonances and the nondiagonal elements the *coherent* superposition of the transition amplitudes since the "decay paths" via the intermediate resonances are no longer distinguishable within the cascade. If the splitting of the levels is much larger than their widths, $\omega_{\alpha J, \alpha' J'} \gg \Gamma_{\alpha J, \alpha' J'}$, the nondiagonal matrix elements vanish, and only matrix elements with $J = J'$ contribute to the overall cascade. This refers to the behavior as expected for two or more isolated levels where the total emission is simply obtained as the incoherent sum of all individual decay cascades.

In contrast, the nondiagonal depolarization factors will be significant if the level splitting becomes negligible when compared with the total widths of the levels, $\omega_{\alpha J, \alpha' J'} \ll \Gamma_{\alpha J, \alpha' J'}$, i.e., for a partial or complete overlap of the intermediate resonances. In this case, the precession of the total angular momentum of each resonance due to the spin-orbit coupling will always reduce the orientation or alignment of the intermediate resonances as determined by the nondiagonal elements of the time-dependent statistical tensors for $J \neq J'$ [25].

B. Angular distribution of the second-step photons

Instead of measuring the two photons in coincidence under different angles, it is typically much easier to just observe the angular distribution of one photon with well-defined energy. We can make use of the photon-photon correlation function (2) in order to derive the angular distribution of either photon by integrating this expression over the angles (θ_u, φ_u) of the other *unobserved* photon. For the angular distribution of the second-step photon γ_2, we then obtain

$$W(\theta_2,\varphi_2) = \sum_{k_i q_i} \sum_{\alpha J, \alpha' J'} \sum_{\bar{p}\bar{L}\bar{p}'\bar{L}' p L p' L'} \rho_{k_i q_i}(\alpha_i J_i) \bar{M}_{\bar{p}\bar{L}} \bar{M}^*_{\bar{p}'\bar{L}'} M_{pL} M^*_{p'L'} (-1)^{L'+J+J_f+J_i+J+\bar{L}}$$
$$\times (2k_i+1)^{-1/2} \begin{Bmatrix} J' & L' & J_f \\ L & J & k_i \end{Bmatrix} \begin{Bmatrix} J' & J_i & \bar{L} \\ J_i & J & k_i \end{Bmatrix} \varepsilon^{\mathrm{det}*}_{k_i 0}(pL, p'L') h_{\alpha J, \alpha' J'} \sqrt{\pi} Y_{k_i q_i}(\theta_2,\varphi_2), \quad (5)$$

where we use the same notations as in Eqs. (2)–(4) above. An interference of the transition amplitudes occurs for the second-step photon due to the coherent excitation of the intermediate resonances, as seen clearly from the multiple product of the transition amplitudes for different decay channels via the resonances.

Let us note that an expression similar to Eq. (5) is found also for the angular distribution of the first-step photon, if the correlation function is integrated over the angles θ_2, φ_2, and by interchanging the labels $\gamma_2 \to \gamma_1$. At first glance, this might be surprising because the angular distribution of the first photon here appears more complex than the standard dipole distribution of atomic photoionization [34] even though the second-step photon remains undetected. This behavior however is due to the known emission of a second photon and has been discussed extensively

in the context of sequential two-photon double ionization [25,26].

C. Two-step photon cascades of lithiumlike ions: Angular distribution and angular correlations

We can apply the expressions (2) and (5) from above to analyze the angular correlation and angular distribution of the two-step radiative cascade

$$\begin{aligned} &1s2p^2\ J_i = 1/2,3/2 \\ &\quad \to \gamma_1 + \begin{Bmatrix} 1s2s2p\ J = 1/2 \\ 1s2s2p\ J' = 3/2 \end{Bmatrix} \\ &\quad \to \gamma_1 + \gamma_2 + 1s^2 2s\ J_f = 1/2 \end{aligned} \tag{6}$$

of lithiumlike ions. Note that all radiative transitions involved here are *electric-dipole*-allowed lines. The angular distribution of the dipole photons is determined only by the second-rank statistical tensors (alignment) $\rho_{2q}(\alpha_i J_i)$. The initial levels $1s2p^2\ J_i = 1/2,3/2$ might be produced by either dielectronic recombination or electron impact excitation. In this case one can choose the quantization z axis along the electron beam direction. Then only one projection $\rho_{20}(\alpha_i J_i)$ of the statistical tensors is nonzero, and the initial level is fully characterized by means of the alignment parameter $\mathcal{A}_2(\alpha_i J_i) = \rho^i_{20}(\alpha_i J_i)/\rho^i_{00}(\alpha_i J_i)$. Below, we always consider such a case. In the following, we shall present examples where only electric-dipole transitions are considered; thus, $p = p' = \bar{p} = \bar{p}' = 0$, and $L = L' = \bar{L} = \bar{L}' = 1$ in Eqs. (2) and (5). Figure 2 displays the radiative cascade (6) schematically, along with the other decay channels from the $1s2p^2\ J_i = 1/2,3/2$ doubly excited levels and the corresponding branching fractions for lithiumlike W^{71+} ions. Therefore, while the doubly excited level of interest predominantly decays via the two $1s^2 2p\ J_f = 1/2,3/2$ levels, about 0.01% of its overall decay proceeds via the cascades (6) and might indeed be explored experimentally.

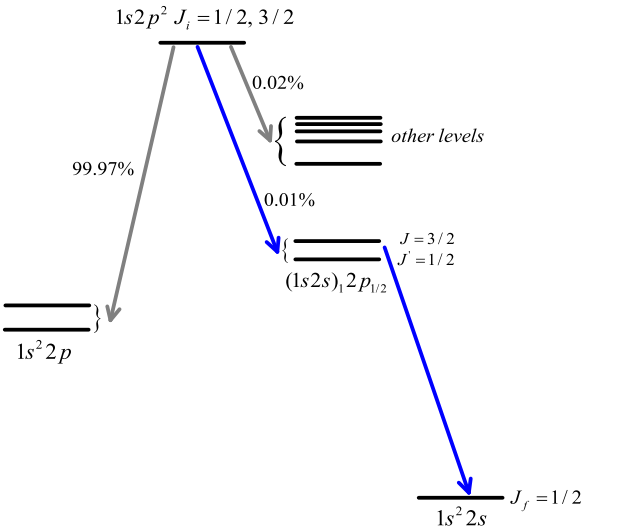

FIG. 2. (Color online) Level scheme and dominant decay channels of the doubly excited $1s2p^2\ J_i = 1/2,3/2$ resonances of lithiumlike W^{71+} ions along with their estimated branching fractions. About 0.01% proceeds via the (blue) radiative cascade (6) of interest.

For the radiative cascade (6) from the initial $J_i = 1/2$ level, the angular correlation function (2) can be expressed in the following normalized form:

$$W^{\gamma_1\gamma_2}_{J_i=1/2}(\Omega_{12}) \propto 1 + \beta^{\gamma_1\gamma_2}_{J_i=1/2} P_2(\cos\Omega_{12}). \tag{7}$$

Here, the second-order Legendre polynomial $P_2(\cos\Omega_{12})$ occurs as a function of the *opening* angle $\cos\Omega_{12} = \cos\theta_1\cos\theta_2 + \sin\theta_1\sin\theta_2\cos(\varphi_1 - \varphi_2)$ between the directions of the two outgoing photons. For the initial $J_i = 1/2$ level, obviously, the nonisotropic emission of the two photons can be parametrized by just the single anisotropy parameter

$$\beta^{\gamma_1\gamma_2}_{J_i=1/2} = \frac{\frac{1}{4}\left|M^{\gamma_1}_{3/2}\right|^2\left|M^{\gamma_2}_{3/2}\right|^2\frac{1}{\Gamma_{3/2}} - \mathrm{Re}\left(M^{\gamma_1}_{1/2}M^{\gamma_1 *}_{3/2}M^{\gamma_2}_{1/2}M^{\gamma_2 *}_{3/2}h_{1/2,3/2}\right)}{\left|M^{\gamma_1}_{3/2}\right|^2\left|M^{\gamma_2}_{3/2}\right|^2\frac{1}{\Gamma_{3/2}} + 2\left|M^{\gamma_1}_{1/2}\right|^2\left|M^{\gamma_2}_{1/2}\right|^2\frac{1}{\Gamma_{1/2}}}. \tag{8}$$

In this formula, we have made use of the shorthand notations $M^{\gamma_1}_J \equiv \langle 1s2s2pJ\|H_{\gamma_1}(E1)\|1s2p^2 J_i = 1/2\rangle$ and $M^{\gamma_2}_J \equiv \langle 1s^2 2s J_f = 1/2\|H_{\gamma_2}(E1)\|1s2s2pJ\rangle$ with $J = 1/2,3/2$ in order to denote the transition amplitudes of the first and second steps of the cascade (6). Re stands for the real part of the corresponding complex term. The depolarization factor $h_{1/2,3/2}$ has the same form as in Eq. (4) and has to be evaluated for the $1s2s2p\ J = 1/2,3/2$ resonances. As seen from this expression, the anisotropy parameter $\beta^{\gamma_1\gamma_2}_{J_i=1/2}$ is independent of the polarization state $\rho_{k_i q_i}(\alpha_i J_i)$ of the initial doubly excited level. This can be easily understood since this level with $J_i = 1/2$ cannot be aligned in the course of any axially symmetric process.

For the initial $1s2p^2\ J_i = 3/2$ resonance, however, it is usually aligned along the direction of the electron beam if it is populated following the electron impact processes. In this case, the corresponding angular correlation function $W^{\gamma_1\gamma_2}_{J_i=3/2}$ depends on three angles θ_1, θ_2, and φ_2 for a special choice of coordinate system with its z axis along the alignment and x axis chosen in such a way that the azimuth angle of the first photon is zero. The photon detectors are usually mounted in the plane perpendicular to the beam; thus $\theta_1 = \theta_2 = 90^\circ$, and the angular correlation function depends on only one angle φ_2. After standard normalization, it can be expressed as follows:

$$W^{\gamma_1\gamma_2}_{J_i=3/2}(\varphi_2) \propto 1 + \beta^{\gamma_1\gamma_2}_{J_i=3/2} P_2(\cos\varphi_2). \tag{9}$$

Here, φ_2 denotes the azimuth angle of the second-step photon, and $\beta^{\gamma_1\gamma_2}_{J_i=3/2}$ is the corresponding anisotropy parameter

$$\beta^{\gamma_1\gamma_2}_{J_i=3/2} = \frac{2(1-\mathcal{A}_2)\left[\sqrt{10}\,\mathrm{Re}\left(M^{\gamma_1}_{1/2}M^{\gamma_1*}_{3/2}M^{\gamma_2}_{1/2}M^{\gamma_2*}_{3/2}h_{1/2,3/2}\right) - 2\frac{|M^{\gamma_1}_{3/2}|^2|M^{\gamma_2}_{3/2}|^2}{\Gamma_{3/2}}\right]}{10(4-\mathcal{A}_2)\frac{|M^{\gamma_1}_{1/2}|^2|M^{\gamma_2}_{1/2}|^2}{\Gamma_{1/2}} + (20+\mathcal{A}_2)\frac{|M^{\gamma_1}_{3/2}|^2|M^{\gamma_2}_{3/2}|^2}{\Gamma_{3/2}} - 3\sqrt{10}\mathcal{A}_2\mathrm{Re}\left(M^{\gamma_1}_{1/2}M^{\gamma_1*}_{3/2}M^{\gamma_2}_{1/2}M^{\gamma_2*}_{3/2}h_{1/2,3/2}\right)}. \tag{10}$$

Again, we here use the same notations as in Eq. (8) apart from the reduced radiative transition amplitudes of the first step, $M^{\gamma_1}_J \equiv \langle 1s2s2pJ\|H_{\gamma_1}(E1)\|1s2p^2J_i = 3/2\rangle$ with $J = 1/2,3/2$. Moreover, the initial $1s2p^2\,J_i = 3/2$ level might be aligned in general owing to its prior excitation process and described here by the alignment parameter $\mathcal{A}_2 = \rho^i_{20}/\rho^i_{00}$ [33,34], as discussed above.

We can use Eq. (5) in order to parametrize the angular distribution of the second-step photons in process (6). For the initial $1s2p^2\ J_i = 1/2$ level, it follows from Eq. (5) that $J = J'$ since it is characterized by just one *zero*-rank statistical tensor ρ^i_{00}, i.e., $k_i = 0$. As a result, only the diagonal elements of the depolarization factor (4) survive, and the angular distribution (5) will be isotropic and not sensitive to the splitting. This case is of course not interesting for our purpose of analyzing the level splitting of HCIs. However, if the radiative cascade starts from the initial $1s2p^2\ J_i = 3/2$ resonance, the *characteristic* angular distribution of the second-step photon depends on the splitting, and it can be given as follows:

$$W^{\gamma_2}_{J_i=3/2}(\theta_2) \propto 1 + \beta^{\gamma_2}_{J_i=3/2}P_2(\cos\theta_2). \tag{11}$$

Here, θ_2 represents the polar angle of the emitted second-step photon with regard to the quantization axis, and it was chosen along the beam of incoming electrons in the prior excitation process. The corresponding anisotropy parameter is given by

$$\beta^{\gamma_2}_{J_i=3/2} = \mathcal{A}_2\frac{\left|M^{\gamma_1}_{3/2}\right|^2\left|M^{\gamma_2}_{3/2}\right|^2\frac{1}{\Gamma_{3/2}} + 4\sqrt{10}\mathrm{Re}\left(M^{\gamma_1}_{1/2}M^{\gamma_1*}_{3/2}M^{\gamma_2}_{1/2}M^{\gamma_2*}_{3/2}h_{1/2,3/2}\right)}{10\left(\left|M^{\gamma_1}_{3/2}\right|^2\left|M^{\gamma_2}_{3/2}\right|^2\frac{1}{\Gamma_{3/2}} + 2\left|M^{\gamma_1}_{1/2}\right|^2\left|M^{\gamma_2}_{1/2}\right|^2\frac{1}{\Gamma_{1/2}}\right)}, \tag{12}$$

and with the same reduced amplitudes and depolarization factor as in Eq. (10). As seen from Eq. (12), the parameter $\beta^{\gamma_2}_{J_i=3/2}$ is directly proportional to the alignment parameter $\mathcal{A}_2$ of the initial, doubly excited $1s2p^2\ J_i = 3/2$ level, and, hence the stronger this alignment the stronger the observed anisotropy of the second-step photons.

D. Evaluation of transition amplitudes

To further explore the photon angular distribution and photon-photon correlation functions in process (6), all that we need to do is to calculate the radiative transition amplitudes $\langle\alpha_f J_f\|H_\gamma(pL)\|\alpha_i J_i\rangle$ in Eqs. (7)–(12). However, since these matrix elements occur rather frequently in the computation of atomic properties, such as transition probabilities, excitation cross sections, and at various places elsewhere [35–39], they can be obtained quite readily from different codes. Here, we follow our previous work in studying the x-ray emission from HCIs [38,39] and employ the multiconfiguration Dirac-Fock (MCDF) method [40–42] to evaluate all the necessary amplitudes. In this MCDF method, an atomic-state wave function with angular momentum J and parity P is approximated by a linear combination of configuration-state functions (CSFs) of the same symmetry,

$$\psi_\alpha(PJM) = \sum_{r=1}^{n_c} c_r(\alpha)|\phi_r(PJM)\rangle, \tag{13}$$

where n_c is the number of CSFs and where $c_r(\alpha)$ denotes the configuration mixing coefficients. Moreover, while the CSFs are constructed self-consistently on the basis of the Dirac-Coulomb Hamiltonian, further relativistic and quantum-electrodynamical effects can be easily incorporated into the representation $c_r(\alpha)$ of the atomic states by diagonalizing the Dirac-Coulomb-Breit Hamiltonian matrix in first-order perturbation theory [43]. In the present work, we have calculated all atomic states and amplitudes as associated with the $1s^22s$, $1s^22p$, $1s2s^2$, $1s2s2p$, and $1s2p^2$ configurations by using the GRASP92 [40] and RATIP codes [41,42], respectively.

III. RESULTS AND DISCUSSION

Equation (2) for the photon-photon angular correlation function and Eq. (5) for the angular distribution of the second-step photons are general and can thus be applied to any two-step radiative cascade with two (or more) overlapping intermediate resonances. We here use these expressions in their particular form (7)–(12) to analyze how sensitively the photon emission in process (6) depends on the level splitting of the intermediate resonances. We choose this particular decay of inner-shell excited, lithiumlike ions since all individual transitions of the cascade (6) are *electric-dipole* allowed, and no other multipoles of the radiation field and their corresponding reduced amplitudes need to be taken into account. Moreover, we here have a level crossing of the two intermediate $1s2s2p_{1/2}\ J = 1/2, 3/2$ resonances along the lithium isoelectronic sequence in the range $74 \leqslant Z \leqslant 79$, which makes these ions interesting for exploring the depolarization effects as a function of the nuclear charge Z. Figure 3 displays the level splitting $\Delta\omega$ of the $1s2s2p_{1/2}\ J = 1/2, 3/2$ resonances as calculated within the MCDF method. Near to the level crossing, of course, the depolarization effects are expected to be largest.

In the following, all computations were performed with the transition amplitudes of lithiumlike W^{71+} ions in order to explore the x-ray emissions from the two-step radiative decay (6) but for a variable level splitting of the intermediate resonances. While the amplitudes depend only weakly on the exact level

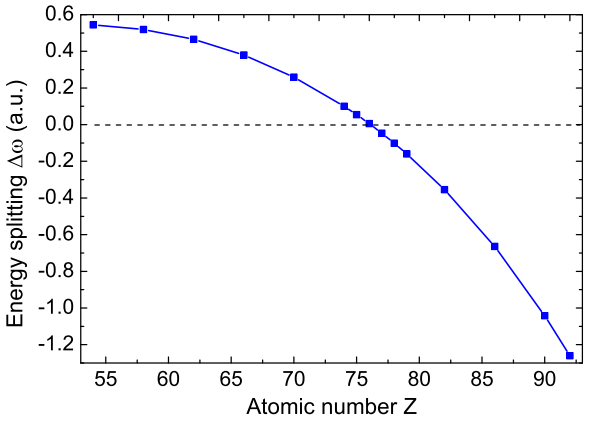

FIG. 3. (Color online) Energy splitting $\Delta\omega$ between the two intermediate $1s2s2p_{1/2}$ $J = 1/2,3/2$ levels as function of the atomic number Z along the lithium isoelectronic sequence. The crossing of these two levels occurs approximately in the range $74 \leqslant Z \leqslant 79$.

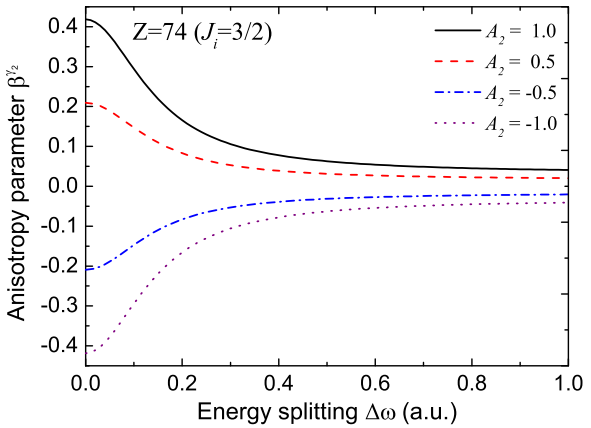

FIG. 4. (Color online) Anisotropy parameters (12) of the angular distribution of the second-step photons as functions of the level splitting $\Delta\omega$. Results are shown for an initially aligned $1s2p^2$ $J_i = 3/2$ resonance of lithiumlike W^{71+} ions and by assuming four different alignment parameters for this resonance owing to its prior excitation: $\mathcal{A}_2 = 1.0$ (black solid line), 0.5 (red dashed lined), -0.5 (blue dash-dotted line), and -1.0 (gray dotted line).

energies and even the nuclear charge, accurate calculations of the level splitting are difficult near the crossing of the levels. Therefore, we here propose two experimental scenarios for determining this splitting either by a measurement of the angular distribution of the second-step photons or by means of a coincident measurement of the photon-photon correlation function.

A. Angular distribution of the second-step photon

How large can the effects of depolarization become upon a single, well-defined line in the x-ray emission spectrum of HCIs? To answer this question, let us consider the angular distribution of the second-step photons from the cascade (6) which is much easier to observe than the two-photon angular correlations in coincidence measurements. However, while the angular distribution of the second-step photon is always isotropic for the unpolarized initial $1s2p^2$ $J_i = 1/2$ level, a strong dependence on the splitting of the two intermediate levels is found for the initially aligned $1s2p^2$ $J_i = 3/2$ resonance.

Figure 4 displays the anisotropy parameters (12) of the second-photon angular distribution as functions of the level splitting $\Delta\omega$ for the initially aligned $1s2p^2$ $J_i = 3/2$ level. Results are shown for lithiumlike W^{71+} ions and for four different alignment parameters as they may arise due to different excitation processes for these doubly excited levels [44]. As seen from this figure, the anisotropy parameter $\beta^{\gamma_2}_{J_i=3/2}$ appears to be very sensitive with regard to the level splitting and, in particular, for all splittings $\Delta\omega \lesssim 0.2$ a.u. ≈ 5.4 eV. Such changes in the anisotropy of the emitted second-step photons can be measured quite easily for HCIs by using present-day detection techniques [45,46]. This requires consideration of the anisotropy parameter $\beta^{\gamma_2}_{J_i=3/2}$ as a function of the nuclear charge since the level splitting is fixed for any given ion. As seen from expression (12), the modifications in the observed anisotropy will be proportional to the alignment of the initial $1s2p^2$ $J_i = 3/2$ resonance.

Figure 5 shows the angular distribution of the second-step photon emission in the cascade (6). Four different level splittings of the intermediate $1s2s2p_{1/2}$ $J = 1/2,3/2$ resonances are assumed here in order to demonstrate the strong influence of the level splitting upon the angular distribution of the observed photons. Obviously, the overall shape of this photon emission depends again on the alignment of the initial $1s2p^2$ $J_i = 3/2$ level, which might be controlled experimentally due to its excitation. This alignment of the initial level can be measured also quite easily by recording the fluorescence of this level to some other *isolated* levels, such as $1s^22p$ $J = 1/2,3/2$, as shown in Fig. 2. Therefore, this rather strong sensitivity of the second-photon angular distribution might make such measurements a suitable tool for determining small level splittings in excited HCIs.

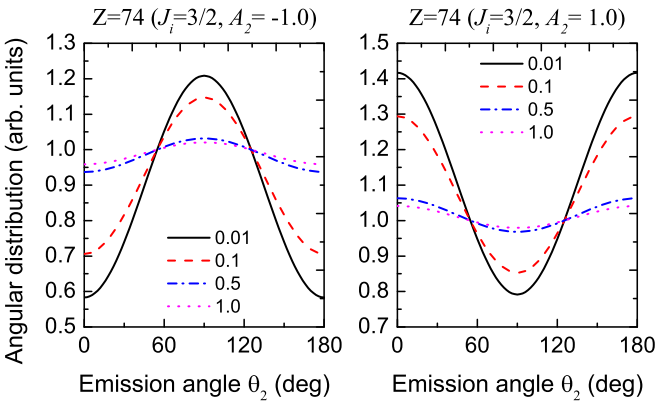

FIG. 5. (Color online) Angular distribution of the second-step photon emission for the cascade (6). Results are shown for an initially aligned $1s2p^2$ $J_i = 3/2$ resonance with alignment parameters $\mathcal{A}_2 = -1.0$ (left panel) and 1.0 (right panel) of lithiumlike W^{71+} ions and for four assumed level splittings of the intermediate $1s2s2p_{1/2}$ $J = 1/2,3/2$ levels: $\Delta\omega = 0.01$ a.u. (black solid line), 0.1 a.u. (red dashed line), 0.5 a.u. (blue dash-dotted line), and 1.0 a.u. (pink dotted line).

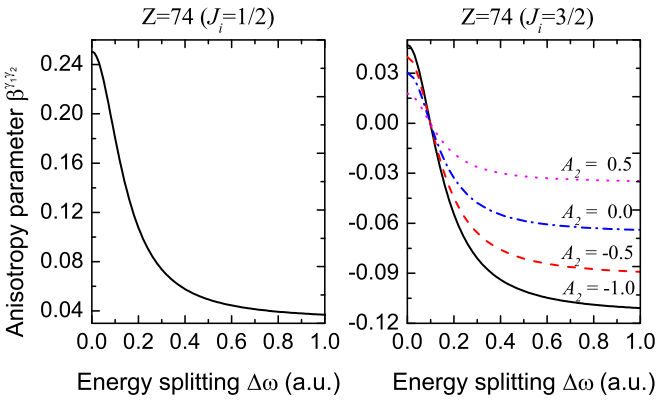

FIG. 6. (Color online) Anisotropy parameters (8) and (10) for the photon-photon angular correlation function of the initial $1s2p^2\ J_i = 1/2$ (left panel) and $1s2p^2\ J_i = 3/2$ (right panel) resonances of lithiumlike W^{71+} ions. These parameters are shown as functions of energy splitting $\Delta\omega$ and for four different alignment parameters of the $J_i = 3/2$ resonance: $\mathcal{A}_2 = -1.0$ (black solid line), -0.5 (red dotted line), 0.0 (blue dash-dotted line), and 0.5 (pink dotted line).

B. Angular correlation between two photons

Apart from just recording the angular distribution of the second-step photons, further details about the cascade (6) and the influence of overlapping resonances can be obtained from the photon-photon correlation function (7) and by measuring the corresponding anisotropy parameter $\beta^{\gamma_1\gamma_2}$. In Fig. 6, we show the dependence of this anisotropy parameter as a function of the energy splitting $\Delta\omega$ of the two intermediate levels. Results are shown for the initial $1s2p^2\ J_i = 1/2$ level of lithiumlike W^{71+} ions (left panel) as well as for four different alignment parameters of the $1s2p^2\ J_i = 3/2$ level (right panel) with $\mathcal{A}_2 = -1.0$, -0.5, 0.0, and 0.5, respectively. For the initial $1s2p^2\ J_i = 1/2$ level, in particular, the photon-photon angular correlation function exhibits a strong anisotropy when compared with the isotropic emission of the second photon alone. A remarkably strong anisotropy is found for all level splittings $\Delta\omega \lesssim 0.2$ a.u. In contrast, the decay of the initial $1s2p^2\ J_i = 3/2$ level results in only a relatively weak angular anisotropy. As seen from the right panel of Fig. 6, moreover, the anisotropy parameter $\beta^{\gamma_1\gamma_2}_{J_i=3/2}$ changes sign at $\Delta\omega \simeq 0.1$ a.u. $\simeq 2.7$ eV and becomes positive for smaller level splitting, i.e., the photon-photon correlation function changes its behavior near the level crossing. This *qualitative* change of the photon-photon angular correlation, in particular, may provide a simple tool to reach a higher level of accuracy in determining the level splitting of HCIs.

This qualitative change in the behavior of the photon-photon angular correlation function is made explicit in Fig. 7, which shows the relative photon angular distribution as a function of the opening angle (for $J_i = 1/2$) and of the azimuth angle φ_2 of the emitted second-step photons (for $J_i = 3/2$). These distributions are shown for the initial $1s2p^2\ J_i = 1/2$ level (left panel) of lithiumlike W^{71+} ions as well as the $1s2p^2\ J_i = 3/2$ level with initial alignment $\mathcal{A}_2 = -1.0$ (middle panel) and 0.0 (right panel) and for the same level splittings as in Fig. 5. As seen clearly, the angular correlation function is very sensitive to the level splitting of the two intermediate levels for both cases. While the smallest level splitting gives rise to the strongest anisotropic angular distribution for the initial $1s2p^2\ J_i = 1/2$ level, the lifetime-induced modification leads to a qualitatively different behavior of x-ray emissions in the case of the $1s2p^2\ J_i = 3/2$ resonance.

IV. CONCLUSION

In summary, general expressions have been derived for the photon-photon angular correlation function as well as for the angular distribution of the individual photons if emitted in the course of a two-step radiative cascade via two (or more) overlapping intermediate resonances. Emphasis has been placed especially on the question of how the level splitting of the overlapping resonances affects the photon emission and how measurements on the photon angular distributions may help to reveal level crossings or to measure explicitly

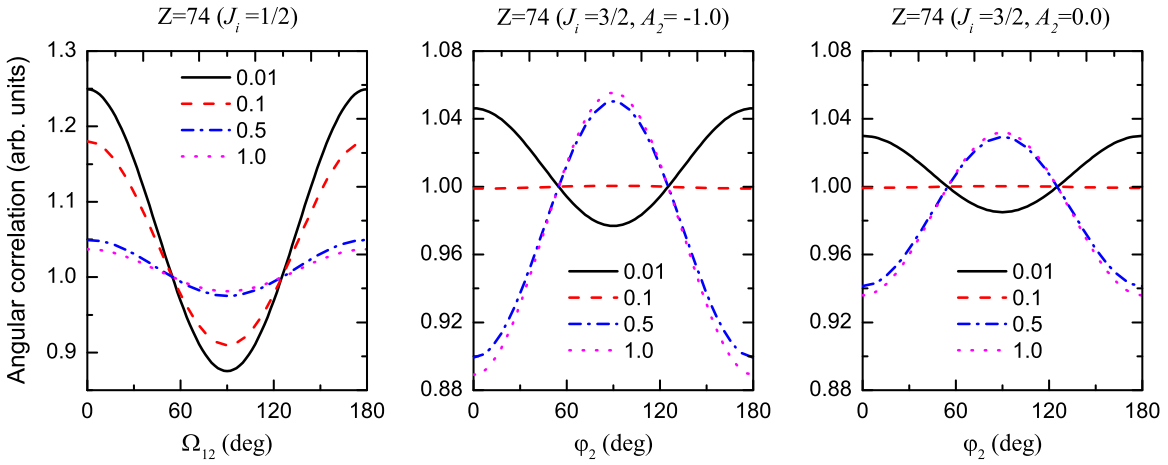

FIG. 7. (Color online) Photon-photon angular correlation functions for the photon cascade (6) are shown here for the initial $1s2p^2\ J_i = 1/2$ level (left panel) calculated using Eq. (7) as well as the $1s2p^2\ J_i = 3/2$ level with initial alignment $\mathcal{A}_2 = -1.0$ (middle panel) and 0.0 (right panel) of lithiumlike W^{71+} ions calculated using Eq. (9). Results are shown for the same level splittings of the intermediate resonances and using the same style as in Fig. 4.

small level splittings of excited HCIs. The derivations of these expressions were carried out in the framework of density matrix theory and calculations performed especially for the core-excited $1s2p^2\ J_i = 1/2,3/2$ levels of ions along the lithium isoelectronic sequence. Apart from a few other strong fluorescence lines, these levels decay also via the intermediate $1s2p^2\ J_i = 1/2,3/2$ resonance, for which a level crossing occurs in the range $74 \leqslant Z \leqslant 79$. For these ions, a strong depolarization effect is found for the angular distribution and angular correlation function for a level splitting $\Delta\omega \lesssim 0.2$ a.u. ≈ 5.4 eV. For the radiative decay of the $1s2p^2\ J_i = 3/2$ resonance, in addition, the initial alignment $\mathcal{A}_2(J_i = 3/2)$ also plays a significant role in the emitted photon distributions; for this resonance, especially, the largest alignment $\mathcal{A}_2 = -1.0$ is expected for the dielectronic recombination of initially heliumlike ions.

From this theoretical analysis, we conclude that accurate measurements of the angular x-ray emission may serve also as a tool for determining small level splittings in highly charged ions. Such measurements of the photon angular distributions are feasible with present-day x-ray detectors and could be carried out at both heavy-ion storage rings and electron beam ion trap facilities.

ACKNOWLEDGMENTS

Z.W.W. acknowledges the support of a research scholarship from the Helmholtz Institute Jena and the Helmholtz Association of Germany. This work has been supported by the BMBF under Contract No. 05K13VHA and by the National Natural Science Foundation of China under Grants No. 11274254 and No. U1332206.

[1] M. A. Levine, R. E. Marrs, J. N. Bardsley, P. Beiersdorfer, C. L. Bennett, M. H. Chen, T. Cowan, D. Dietrich, J. R. Henderson, D. A. Knapp, A. Osterheld, B. M. Penetrante, M. B. Schneider, and J. H. Scofield, Nucl. Instrum. Methods Phys. Res., Sect. B **43**, 431 (1989).

[2] M. Schulz, C. L. Cocke, S. Hagmann, M. Stöckli, and H. Schmidt-Böcking, Phys. Rev. A **44**, 1653 (1991).

[3] P. Beiersdorfer, R. E. Olson, G. V. Brown, H. Chen, C. L. Harris, P. A. Neill, L. Schweikhard, S. B. Utter, and K. Widmann, Phys. Rev. Lett. **85**, 5090 (2000).

[4] D. B. Thorn, M. F. Gu, G. V. Brown, P. Beiersdorfer, F. S. Porter, C. A. Kilbourne, and R. L. Kelley, Phys. Rev. Lett. **103**, 163001 (2009).

[5] A. H. Gabriel, Mon. Not. R. Astron. Soc. **160**, 99 (1972).

[6] K. Honda, K. Mima, and F. Koike, Phys. Rev. E **55**, 4594 (1997).

[7] I. Martinson, Rep. Prog. Phys. **52**, 157 (1989); Nucl. Instrum. Methods Phys. Res., Sect. B **43**, 323 (1989).

[8] I. Martinson and L. J. Curtis, Contemp. Phys. **30**, 173 (1989).

[9] J. D. Gillaspy, J. Phys. B **34**, R93 (2001).

[10] J. Eichler and W. Meyerhof, *Relativistic Atomic Collisions* (Academic Press, San Diego, 1995).

[11] G. A. Machicoane, T. Schenkel, T. R. Niedermayr, M. W. Newmann, A. V. Hamza, A. V. Barnes, J. W. McDonald, J. A. Tanis, and D. H. Schneider, Phys. Rev. A **65**, 042903 (2002).

[12] S. Fritzsche, A. Surzhykov, A. Gumberidze, and T. Stöhlker, New J. Phys. **14**, 083018 (2012).

[13] Z. W. Wu, C. Z. Dong, and J. Jiang, Phys. Rev. A **86**, 022712 (2012).

[14] J. M. Bizau, J. M. Esteva, D. Cubaynes, F. J. Wuilleumier, C. Blancard, A. C. La Fontaine, C. Couillaud, J. Lachkar, R. Marmoret, C. Rémond, J. Bruneau, D. Hitz, P. Ludwig, and M. Delaunay, Phys. Rev. Lett. **84**, 435 (2000).

[15] S. Fritzsche, P. Indelicato, and Th. Stöhlker, J. Phys. B **38**, S707 (2005).

[16] M. S. Pindzola, Sh. A. Abdel-Naby, F. Robicheaux, and J. Colgan, Phys. Rev. A **85**, 032701 (2012).

[17] J. R. Henderson, P. Beiersdorfer, C. L. Bennett, S. Chantrenne, D. A. Knapp, R. E. Marrs, M. B. Schneider, K. L. Wong, G. A. Doschek, J. F. Seely, C. M. Brown, R. E. LaVilla, J. Dubau, and M. A. Levine, Phys. Rev. Lett. **65**, 705 (1990).

[18] R. Bensaid, M. K. Inal, and J. Dubau, J. Phys. B **39**, 4131 (2006).

[19] S. Fritzsche, A. Surzhykov, and Th. Stöhlker, Phys. Rev. Lett. **103**, 113001 (2009).

[20] Z. M. Hu, X. Y. Han, Y. M. Li, D. Kato, X. M. Tong, and N. Nakamura, Phys. Rev. Lett. **108**, 073002 (2012).

[21] Z. W. Wu, J. Jiang, and C. Z. Dong, Phys. Rev. A **84**, 032713 (2011).

[22] A. Surzhykov, Y. Litvinov, Th. Stöhlker, and S. Fritzsche, Phys. Rev. A **87**, 052507 (2013).

[23] Z. W. Wu, A. Surzhykov, and S. Fritzsche, Phys. Rev. A **89**, 022513 (2014).

[24] N. M. Kabachnik, S. Fritzsche, A. N. Grum-Grzhimailo, M. Meyer, and K. Ueda, Phys. Rep. **451**, 155 (2007).

[25] E. V. Gryzlova, A. N. Grum-Grzhimailo, S. Fritzsche, and N. M. Kabachnik, J. Phys. B **43**, 225602 (2010).

[26] S. Fritzsche, A. N. Grum-Grzhimailo, E. V. Gryzlova, and N. M. Kabachnik, J. Phys. B **41**, 165601 (2008); **44**, 175602 (2011).

[27] K. Ueda, Y. Shimizu, H. Chiba, Y. Sato, M. Kitajima, H. Tanaka, and N. M. Kabachnik, Phys. Rev. Lett. **83**, 5463 (1999).

[28] K. Ueda, Y. Shimizu, H. Chiba, M. Kitajima, H. Tanaka, S. Fritzsche, and N. M. Kabachnik, J. Phys. B **34**, 107 (2001).

[29] K. Ueda, Y. Shimizu, H. Chiba, M. Kitajima, M. Okamoto, M. Hoshino, H. Tanaka, T. Hayaishi, S. Fritzsche, I. P. Sazhina, and N. M. Kabachnik, J. Phys. B **36**, 319 (2003).

[30] J. Eichler, A. Ichihara, and T. Shirai, Phys. Rev. A **58**, 2128 (1998).

[31] J. H. Scofield, Phys. Rev. A **44**, 139 (1991).

[32] E. G. Drukarev, X. Ma, A. I. Mikhailov, I. A. Mikhailov, and P. H. Mokler, Phys. Rev. A **74**, 022717 (2006).

[33] K. Blum, *Density Matrix Theory and Applications* (Plenum, New York, 1981).

[34] V. V. Balashov, A. N. Grum-Grzhimailo, and N. M. Kabachnik, *Polarization and Correlation Phenomena in Atomic collisions* (Kluwer Academic, New York, 2000).

[35] I. P. Grant, Adv. Phys. **19**, 747 (1970).

[36] I. P. Grant, J. Phys. B **7**, 1458 (1974).

[37] M. K. Inal, A. Surzhykov, and S. Fritzsche, Phys. Rev. A **72**, 042720 (2005).

[38] A. Surzhykov, U. D. Jentschura, Th. Stöhlker, and S. Fritzsche, Phys. Rev. A **73**, 032716 (2006).

[39] S. Fritzsche, A. Surzhykov, and Th. Stöhlker, Phys. Rev. A **72**, 012704 (2005).
[40] F. A. Parpia, C. F. Fischer, and I. P. Grant, Comput. Phys. Commun. **94**, 249 (1996).
[41] S. Fritzsche, Comput. Phys. Commun. **183**, 1525 (2012).
[42] S. Fritzsche, J. Electron Spectrosc. Relat. Phenom. **114–116**, 1155 (2001).
[43] S. Fritzsche, C. F. Fischer, and G. Gaigalas, Comput. Phys. Commun. **148**, 103 (2002).
[44] Such an alignment of the initial $1s2p^2\ J_i = 3/2$ resonance is typically produced in all ion-atom or ion-electron collisions. For the dielectronic recombination of initially heliumlike ions, an alignment parameter $\mathcal{A}_2 = -1.0$ is expected for these doubly excited levels if not populated also by other processes.
[45] G. Weber, H. Bräuning, A. Surzhykov, C. Brandau, S. Fritzsche, S. Geyer, S. Hagmann, S. Hess, C. Kozhuharov, R. Märtin, N. Petridis, R. Reuschl, U. Spillmann, S. Trotsenko, D. F. A. Winters, and Th. Stöhlker, Phys. Rev. Lett. **105**, 243002 (2010).
[46] X. Ma, P. H. Mokler, F. Bosch, A. Gumberidze, C. Kozhuharov, D. Liesen, D. Sierpowski, Z. Stachura, Th. Stöhlker, and A. Warczak, Phys. Rev. A **68**, 042712 (2003).